Biosensors and Bioelectronics 77 (2016) 845–852

Contents lists available at ScienceDirect

Biosensors and Bioelectronics

journal homepage: www.elsevier.com/locate/bios

Electrochemiluminescence on digital microfluidics for microRNA analysis

Mohtashim H. Shamsi [a,b,1], Kihwan Choi [a,b,2], Alphonsus H.C. Ng [a,b,c], M. Dean Chamberlain [a,b], Aaron R. Wheeler [a,b,c,*]

[a] Department of Chemistry, University of Toronto, 80 St George St., Toronto, ON, Canada M5S 3H6
[b] Donnelly Centre for Cellular and Biomolecular Research, 160 College St., Toronto, ON, Canada M5S 3E1
[c] Institute of Biomaterials and Biomedical Engineering, University of Toronto, 164 College St., Toronto, ON, Canada M5S 3G9

ARTICLE INFO

Article history:
Received 31 July 2015
Received in revised form
8 October 2015
Accepted 12 October 2015
Available online 22 October 2015

Keywords:
Electrochemiluminescence
Digital microfluidics
MicroRNA
Single nucleotide mismatch
Tumor cells

ABSTRACT

Electrochemiluminescence (ECL) is a sensitive analytical technique with great promise for biological applications, especially when combined with microfluidics. Here, we report the first integration of ECL with digital microfluidics (DMF). ECL detectors were fabricated into the ITO-coated top plates of DMF devices, allowing for the generation of light from electrically excited luminophores in sample droplets. The new system was characterized by making electrochemical and ECL measurements of soluble mixtures of tris(phenanthroline)ruthenium(II) and tripropylamine (TPA) solutions. The system was then validated by application to an oligonucleotide hybridization assay, using magnetic particles bearing 21-mer, deoxyribose analogues of the complement to microRNA-143 (miRNA-143). The system detects single nucleotide mismatches with high specificity, and has a limit of detection of 1.5 femtomoles. The system is capable of detecting miRNA-143 in cancer cell lysates, allowing for the discrimination between the MCF-7 (less aggressive) and MDA-MB-231 (more aggressive) cell lines. We propose that DMF-ECL represents a valuable new tool in the microfluidics toolbox for a wide variety of applications.

1. Introduction

Electrochemiluminescence (ECL) detection has recently emerged as a hot topic in analytical chemistry (Hu and Xu, 2010; Miao, 2008; Mirasoli et al., 2014; Muzyka, 2014; Nepomnyashchii et al., 2006; Parveen et al., 2013; Radha and Mark, 2007; Richter, 2004; Robert et al., 2009; Yin et al., 2004). In ECL, electrically excited chemical species are generated at an electrode surface by applying a electrical potential; those species or their products subsequently emit light to be detected, often in visible region of the spectrum (Miao, 2008). This process makes ECL highly selective, as there are relatively few analytes that are both (a) electroactive, and (b) capable of radiative electronic relaxation. Detection with ECL has multiple advantages, including (1) low background optical signal, (2) precise control over the position and moment of emission (i.e., emission occurs in proximity of electrode surface when an appropriate potential is applied), (3) selective control over which species are addressed (Wang et al., 2012), (4) compatibility with in-solution and in-thin-film emission, and (5) wide dynamic range (3–6 orders of magnitude). ECL luminophores are stable and can be used as selective non-radioactive labels in bioassays with zeptomole sensitivity (Sardesai et al., 2011), and for multi-modal analysis with electrochemical detection (Redha et al., 2009). These advantages have driven the development of commercial ECL systems which have been applied to immunoassays, DNA assays, detection of water-borne parasites, monitoring of environmental hazards, and biowarfare agent detection (ORIGEN®, I.I., Gaithersburg, MD, Elecsys®, Roche Diagnostics, Indianapolis, IN, NucliSens®, Organon Teknika, Durham, NC, and QPCR® 5000, PerkinElmer, Wellesley, MA). ECL has also been incorporated as a detection mode in wide range of analytical tools such as capillary electrophoresis (CE) (Cao et al., 2002), flow injection analysis (FIA) (Zhang et al., 2013), high performance liquid chromatography (HPLC) (Skotty et al., 1996), and microfluidics and micro total analysis systems (μTAS) (Arora et al., 2001).

Microfluidic analytical platforms are promising because of their compatibility with integration, compactness, fast analysis, low reagent and/or sample consumption, and the capacity for multiplexed analysis (Rackus et al., 2015). However, microfluidic platforms are often fundamentally signal-limited because their low

* Corresponding author at: Department of Chemistry, University of Toronto, 80 St George St., Toronto, ON, Canada M5S 3H6. Fax: +416 946 3865.
E-mail address: aaron.wheeler@utoronto.ca (A.R. Wheeler).
[1] Current address: Department of Chemistry and Biochemistry, Southern Illinois University at Carbondale, 1245 Lincoln drive, Carbondale, IL, 62901, USA.
[2] Current address: Division of Metrology for Quality of Life, Korea Research Institute of Standards and Science, Yuseong-gu, Daejeon 305-340, Korea

http://dx.doi.org/10.1016/j.bios.2015.10.036
0956-5663/

sample volumes often contain only few molecules of analyte. Thus, ECL and microfluidics are a natural fit; together, they can be used to detect small amounts of analyte in low sample volumes (Mirasoli et al., 2014). As an example, there is great promise for using ECL for nucleic acid analysis, often implemented using magnetic particles that are modified with complementary oligonucleotide probes. But such assays are tedious, requiring long processing regimens including particle conditioning and blocking, hybridization with sample, extensive wash-steps, mixing with ECL luminophores and co-reactants, and (finally) detection. There have been a number of microfluidic systems combined with ECL detection described in the literature, some relying on enclosed microchannels (Azimi et al., 2011; Hsueh et al., 1996, 1998; Sardesai et al., 2013; Silverbrook et al., 2011), and others relying on lateral flow in paper or other absorptive media (Delaney et al., 2011; Ge et al., 2012; Liu et al., 2015; Mani et al., 2013; Wang et al., 2012; Yan et al., 2013; Guan et al., 2016), but we are unaware of any system that has been developed which integrates all of the steps required for magnetic-particle-based nucleic acid analyses.

Here, we report the first integration of ECL detection with a mode of microfluidics known as digital microfluidics (DMF). DMF is a powerful liquid handling platform that is useful for maneuvering (i.e., move, dispense, mix, and split) discrete droplets on an array of insulated electrodes (Choi et al., 2012). Like other forms of microfluidics, DMF is intrinsically compatible with a variety of analytical detection modalities, including mass spectrometry (Lafrenière et al., 2014), colorimetry (Choi et al., 2015), and electrochemical analysis (Dryden et al., 2013). But DMF is quite distinct from other forms of microfluidics (e.g., there are no channels), and it has never before been combined with electrochemiluminescence. Here, we report a DMF-ECL system applied to a magnetic particle-based nucleic acid hybridization assay using sample volumes of ~1.8 μL. The system was validated by application to analysis of microRNA (miRNA) expression levels that are associated with cancer phenotype (Calin and Croce, 2006). We propose that the coupling between DMF and ECL represents a useful new addition to the analyst's toolbox, with particular utility in the emerging area of miRNA analysis (Labib and Berezovski, 2015; Woolley, 2015).

2. Materials and methods

2.1. Supplementary methods

Methods for immobilization of probe sequence on magnetic particles, as well as DMF device fabrication, assembly, and operation are described in detail in the Supplementary Information.

2.2. Reagents and materials

All reagents were purchased from Sigma Chemical (Oakville, ON, Canada) or Fisher Scientific Canada (Ottawa, ON, Canada) unless otherwise specified. Analytical grade reagents were used to prepare solutions of 0.3 M $AgNO_3$ in 3 M NH_4OH, 2.0 mM $KAuCl_4$ in 0.5 M H_2SO_4, 200 μM tris(phenanthroline)ruthenium(II) chloride ($[Ru(Phen)_3]Cl_2$) in phosphate buffered saline, PBS (1 ×), and 20 mM tripropylamine (TPA) in (1 ×). All aqueous solutions were prepared using deionized (DI) water with a resistivity of 18 MΩ●cm at 25 °C. Dynabeads® M-280 Streptavidin were purchased from Invitrogen Dynal AS (Oslo, Norway) as a suspension of 10 mg/mL (~6–7 × 10^8) streptavidin-coated magnetic particles (dia. 2.8 μm) in PBS, containing 0.1% bovine serum albumin (BSA) and 0.02% NaN_3. Binding and washing buffer, B&W (2 ×), was prepared, comprising 10 mM Tris–HCl (pH 7.5) containing 1 mM ethylenediaminetetraacetic acid (EDTA) and 2 M NaCl, and diluted to B&W (1 ×) in DI water. Hybridization buffer (pH 8.0) was prepared, comprising 20 mM Tris–HCl containing 0.2 M NaCl and 5 mM $MgCl_2$. HPLC-purified biotinylated probe DNA sequence and target DNA sequences (Table S1 in the supplementary information) were purchased from Bio Basic Canada Inc. (Markham, ON, Canada). Stock solutions (50 μM) of biotinylated probe DNA sequence and target sequences were prepared in DNase/RNase-free ultrapure water (Invitrogen, Life Technologies, Toronto) and hybridization buffer, respectively. Working solutions from the stock were prepared in the respective medium. All solutions/suspensions were supplemented with Pluronic F68 (0.05% v/v) prior to use with DMF (Au et al., 2011).

2.3. Nucleic acid assay

A seven-step protocol was developed to enable magnetic particle-based nucleic acid assays on DMF. Prior to each analysis, 4.5 μL aliquots of magnetic particle suspension, target sequence solution (0, 10, 100, or 1000 nM ds-143; or 1000 nM 143-m1, 1000 nM 143-m2, or 1000 nM nc-145), hybridization buffer, 200 μM $[Ru(Phen)_3]Cl_2$ solution, PBS, and 20 mM TPA solution were loaded into reservoirs on a device. After all reagents were loaded, (1) three unit droplets containing magnetic particles were dispensed from their reservoir and merged, and the particles were separated from the supernatant. (2) Two unit droplets of target sequence solution were dispensed, merged, and delivered to the immobilized particles for resuspension and incubation for 15 min. (3) The particles were washed four times in series by re-suspending and mixing with one unit droplet of hybridization buffer followed by magnetic separation from the supernatant. (4) Two unit droplets of $[Ru(Phen)_3]Cl_2$ solution were dispensed, merged, and delivered to the particles, where they were re-suspended and mixed for 2 min. The particles were then separated from the supernatant droplet. (5) The particles were washed two times with 2 droplets of PBS as in step 3. (6) Two droplets of TPA solution were dispensed, merged, and delivered to the particles, where they were re-suspended and mixed for 1 min. (7) The final droplet containing TPA and $Ru(Phen)_3^{2+}$-labeled DNA modified particles was actuated to the ECL electrodes on the top-plate for ECL measurements.

2.4. Electrochemistry and electrochemiluminescence

Prior to each assay, cathodic electrochemical cleaning of the ITO WEs was performed to remove adsorbed organic molecules and reduce oxide layer. For this, cyclic voltammetry was performed in 20 μL aliquots of PBS (1 ×) positioned on DMF top plates using the ITO WE and Ag/Au/ITO CE/RE in 10 cycles over a range from –1 V to 0 V with a scan rate of 100 mV/s. In preliminary work, ECL cells were characterized in assembled DMF devices by cyclic voltammetry of a merged droplet formed from dispensed unit droplets of 200 μM $[Ru(Phen)_3]Cl_2$ solution and 20 mM TPA solution. In these experiments, potentials were swept between 0 and 1.8 V at a scan rate of 100 mV/s. ECL cells were also characterized by electrochemiluminescence using the same reagents by applying 1.5 V for 45 s to the ITO WE relative to the Ag/Au/ITO CE/RE, with luminescence collected by the integrated photomultiplier tube (PMT; see Supplementary Information) over that duration. In oligonucleotide assays (described above), the maximum observed ECL signal was recorded for quantitation. In quantitative assays, data were plotted as a function of concentration and fit using a four-parameter logistic regression. The concentration limit of detection (C_{LOD}) was the concentration from the regression equivalent to that of the signal of the blank value plus three standard deviations of the blank. The absolute limit of detection (LOD) was calculated as (C_{LOD}) × (1.8 μL). Statistical significance was

evaluated by Student's *t*-Test.

2.5. Cell culture and analysis

Cell culture reagents were from Life Technologies (Carlsbad, CA). MCF-7 and MDA-MB-231 cell lines were from ATCC (Manassas, VA) and were grown in Dulbecco's modified Eagle medium (DMEM) containing 100 U/mL penicillin G and 100 μg/mL streptomycin supplemented with 10% fetal bovine serum (FBS) in a humidified incubator at 37 °C with 5% CO_2, passaging every 2–3 days. Prior to analysis, cells were trypsinized in 0.25% trypsin-EDTA for 5 min at 37 °C, counted using a hemocyometer, centrifuged at 300 × g for 5 min, and lysed in sufficient volume of RLT buffer (Qiagen, Frederick, MD) to form a mixture equivalent to 10^6 cells mL^{-1}. This suspension was homogenized using a 22 gauge needle, and stored at −20 °C until use. For on-chip assays, MCF-7 lysate, MDA-MB-231 cell lysate, or RTL buffer with no lysate (background solution) was diluted 1:10 in sample dilution buffer (pH 8.0), which was formed from Tris-base (7.7 mM), Tris–HCl (12.2 mM), NaCl (200 mM), $MgCl_2$ (5 mM), and supplemented with BSA (4% w/v) and Pluronic L64 (0.05% w/v). Assays were carried out using the seven-step process described above, except that five unit droplets of magnetic particle suspension were dispensed and merged (in place of three droplets) in step (1).

3. Results and discussion

3.1. Integration of DMF and ECL

Digital microfluidics has recently emerged as a powerful technique for implementing magnetic-bead-based assays (Kokalj et al., 2015), the precise, programmable control making it a perfect fit for automating the many tedious wash, mix, and analysis steps. This combination (DMF and magnetic particles) has been used for a wide range of applications coupled with detection by electrochemistry (Shamsi et al., 2014), fluorescence (Foudeh et al., 2015; Tsaloglou et al., 2014), chemiluminescence (Ng et al., 2012, 2015), and bioluminescence (Welch et al., 2011). But until now, digital microfluidics has never been combined with the promising technique of electrochemiluminescence (ECL) detection. Here, we report our work exploring the suitability of ECL for DMF, with application to magnetic-particle based nucleic acid assays.

As described in the supplementary information, a custom DMF device top-plate (Fig. 1a) was designed for integrated ECL detection, adapted from a design reported previously for electrochemical analysis (Shamsi et al., 2014) with several significant alterations. First, in the current design, the analysis electrodes were moved to the center of the device, appropriate for detection using a PMT positioned above the device. Second, the apertures of the ECL electrodes were designed to be larger than what was reported previously (Shamsi et al., 2014) to allow for increased surface-area for luminophore generation (for increased sensitivity). Third, each working electrode (WE) was formed from bare (transparent) ITO [rather than gold (Shamsi et al., 2014)] to allow for convenient optical detection [note that ITO WEs have been extensively employed for generating ECL in microchannel devices (Kasahara et al., 2014; Wu et al., 2015)]. Fourth, each silver-coated counter/pseudoreference electrode (CE/RE) was formed using a new protocol involving a gold adhesion layer for enhanced mechanical stability. As with the design reported previously for electroanalysis (Shamsi et al., 2014), each analysis electrode was connected to a contact pad, and the remainder of the ITO on the top plate functions as a ground for DMF droplet actuation. The ECL electrodes are sufficiently small such that they do not interfere with droplet movement. Fig. 1b depicts a fully assembled DMF

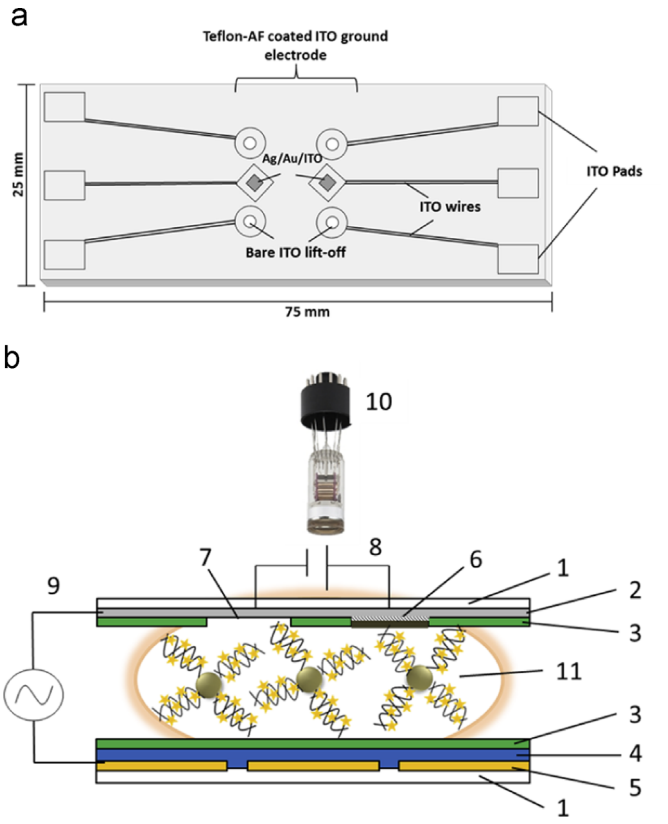

Fig. 1. Digital microfluidics and electrochemiluminescence. (a) Top-view schematic of device top-plate with four bare circular ITO electrodes (dia. 800 μm) that serve as ECL working electrodes (WE) and two square Ag/Au/ITO electrodes (560 μm × 560 μm) that serve as ECL counter/pseudoreference electrodes (CE/RE). The substrate is globally coated with Teflon-AF, with apertures formed above each WE and CE/RE. The ECL electrodes are connected to contact pads through patterned ITO wires, and the remainder of the ITO functions as a ground electrode for DMF operation. (b) Cross-section schematic of two-plate digital microfluidic system for ECL detection. (1) Glass substrate (white), (2) Indium tin oxide (ITO) layer (gray), (3) Teflon-AF hydrophobic layer (green), (4) Parylene-C dielectric layer (blue), (5) Chromium array of DMF driving electrodes (yellow), (6) Ag/Au/ITO CE/RE, (7) Bare ITO WE, (8) Working and counter/psuedoreference electrodes connected via a potentiostat, (9) Top-plate DMF ground electrode and bottom-plate DMF driving electrodes connected via an open-source droplet control system (Fobel et al., 2013), (10) Photomultiplier tube over the top-plate, (11) Droplet containing magnetic beads modified with hybridized DNA oligomers with intercalating labels.

device where top and bottom plates are biased by AC voltages for droplet movement, and DC voltages are applied between the ITO WE and the Ag/Au/ITO CE/RE on the top-plate via a potentiostat. A droplet is shown between the two plates containing magnetic particles modified with labeled double-stranded DNA oligonucleotides. ECL photons are detected by a PMT, which is suspended above the device.

The new DMF-ECL platform was validated using a popular reactant-mixture comprising a ruthenium-based luminophore and tripropylamine (TPA) as a co-reactant. In this system, the luminophore and TPA are oxidized simultaneously, after which TPA^+ reacts further to form an energetically excited radical, which subsequently reduces the luminophore into an energetically excited species that (finally) emits photons, returning to the reactant state (Miao et al., 2002). Here, we used $Ru(Phen)_3^{2+}$ as the luminophore because of its well-known DNA intercalation propensity [i.e., each $Ru(Phen)_3^{2+}$ ion can intercalate into four base pairs in a DNA double helix]. Because soluble $Ru(Phen)_3^{2+}$ does not interact with single-stranded DNA or RNA (Xu and Bard, 1995), this reactant serves as a marker for the amount of double-stranded DNA present in the sample being analyzed, and thus is useful for hybridization assays (Chen et al., 2012; Li et al., 2013; Liu et al.,

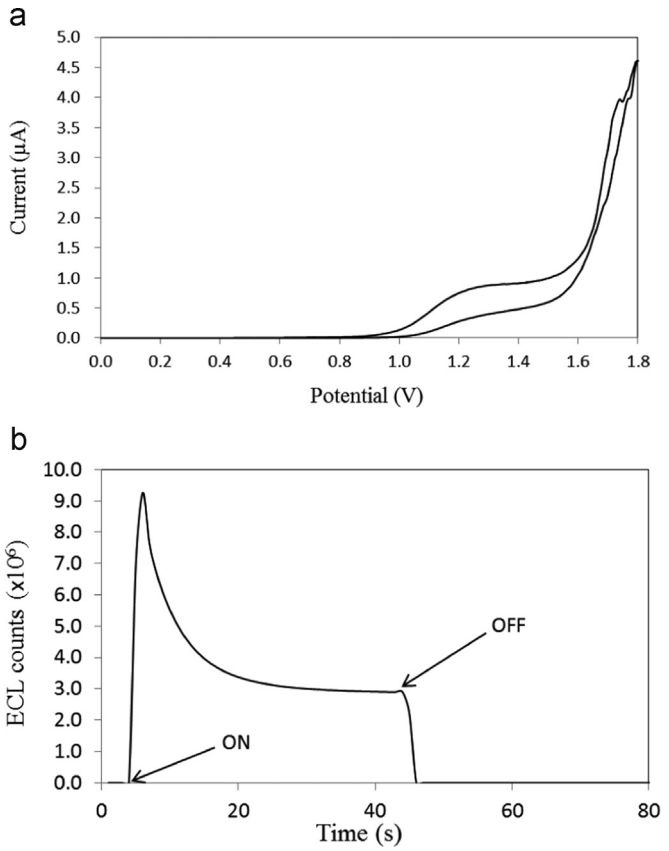

Fig. 2. Characterization of DMF-ECL devices. Representative (a) cyclic voltammogram (swept from 0 to 1.8 V at 100 mV/s on ITO WE vs Ag/Au/ITO CE/RE) and (b) ECL response as a function of time (where "ON" and "OFF" were the times at which 1.5 V as applied and then removed) for a 1:1 mixture of 200 μM $[Ru(Phen)_3]^{2+}$ and 20 mM TPA in PBS buffer (pH 7.4).

2011; Yin et al., 2009).

In initial work, the DMF-ECL detection system was characterized with $Ru(Phen)_3^{2+}$/TPA with no DNA present. Fig. 2a is a representative cyclic voltamogram for this mixture; as shown, there is a broad irreversible anodic peak at ~1.3 V, corresponding to the oxidations of $Ru(Phen)_3^{2+}$ and TPA, reaching a plateau at 1.4–1.5 V [this behavior has been reported elsewhere using a similar reactant mixture (Chiang and Whang, 2001)]. Thus, 1.5 V was chosen as the bias potential for the ECL measurements described here [as reported earlier (Xu and Bard, 1995)]. The system was then characterized by measuring the electroluminescence as a function of time. Fig. 2b shows a representative response, where "ON" and "OFF" represent the times at which 1.5 V was applied (and removed) between the ITO WE and the Ag/Au/ITO CE/RE. In ECL, the oxidative-reductive process theoretically regenerates the luminophore/co-reactant couple at the electrode surface, allowing luminescence to continue at constant value with time. As shown, the luminescence observed here was not constant, and in fact decayed over time. This behavior has been reported previously (Xu and Bard, 1995), likely caused by irreversible decomposition of the luminophore. Regardless, it was found that the maximum luminescence signal, which was observed within 10 s of applying the potential, gave reproducible signals (with coefficient of variance, CV, of 10%). This parameter (the maximum signal observed within 10 s) was used for all experiments with nucleic acids (described below).

A number of parameters were considered in determining the ECL-analysis procedure described here. First, there was some concern that the surfactant used to reduce fouling of the Teflon-AF surface (Au et al., 2011) might interfere with analysis, but this did not prove to be a problem for the procedures described here. Likewise, ruthenium/TPA ECL is a pH-dependent process showing highest intensity when the reactants are dissolved in a buffer with slightly alkaline medium (Miao, 2008); thus, the solutions used here were formed in PBS buffer with pH 7.5. Finally, there are a number of parameters that were not optimized, including working electrode size (800 μm was the only dimension tested) and optical filtering (no filters were used). In the future, if enhanced sensitivity is desirable, users might consider using larger WE areas (as larger electrodes should yield more contact between the electrode and luminophore/coreactant molecules) to allow for more rapid regeneration, and band-pass filters to isolate photons at 540–700 nm (Tokel-Takvoryan et al., 1973) to improve signal to noise ratio.

Finally, we acknowledge that the instrument used to program droplet movement and detect ECL is not (yet) fully integrated. As described in the supplementary information, the custom-made DMF/magnet/PMT system used here is enclosed in the form factor of a large shoebox (Choi et al., 2013), but the commercial potentiostat used for electrochemistry and ECL measurements described here is separate. In the future, to enhance portability and robustness, we propose that it will be straightforward to integrate a DMF-compatible potentiostat (Dryden and Wheeler, 2015) into the enclosed system without any sacrifice in form factor.

3.2. Integrated nucleic acid assays on DMF-ECL

Equipped with a working DMF-ECL prototype system, we applied it to developing an automated assay for oligonucleotide hybridization. Motivated by the enthusiasm for measuring miRNA levels as prognostic markers for cancer (Calin and Croce, 2006), magnetic particles were modified via avidin-biotin chemistry with a 21-mer DNA analogue (ss-143) of the complement to miRNA-143, a molecule that is down-regulated in some tumors (Ng et al., 2009). As outlined in Table S1 in the supplementary information, ds-143 (a synthetic deoxyribose analogue of miRNA-143) was used as a model analyte, and variants of the analyte bearing single- (143-m1) and double- (143-m2) nucleotide mismatches were used to test the specificity of the system. Finally, a fully non-complementary oligonucleotide (nc-145) was used as a negative control. The sequence of nc-145 was chosen such that it is the deoxyribose analogue of another common miRNA found in cancer cells, miRNA-145, making it a representative interferant that is often found in real samples.

A seven-step protocol, depicted in Fig. 3a, was designed and optimized to quantify the level of analyte hybridization to the immobilized ss-143. Fig. 3b shows frames from a movie depicting the steps involved in the new protocol. Briefly, first, ss-143-modified particles were dispensed onto the actuation electrodes followed by magnetic separation of the particles (frames 1&2). Then, particles were incubated with a target sequence droplet followed by repeated wash steps (frames 3&4). The particles were then incubated with $Ru(Phen)_3^{2+}$ solution and washed again (frames 5&6), then mixed with TPA solution (frame 7). The final suspension was driven toward the ITO (WE) and Ag/Au/ITO (CE/RE) to measure the electrochemiluminescence (frame 8). In practice, two assays were commonly implemented in parallel, which required approximately 40 min to complete.

The new assay was applied to a solution of ds-143, and a typical ECL vs. time response is shown in Fig. 4a. The shape of the curve (with a peak followed by a sharp decrease) is different than that observed for free solution (Fig. 2b), because in the hybridization assay, the luminophore is bound to the beads and cannot be regenerated at the electrode. Replicate assays were carried out to evaluate the signal observed for droplets containing the blank solution (no DNA), or 1 μM ds-143, 143-m1, 143-m2, or nc-145.

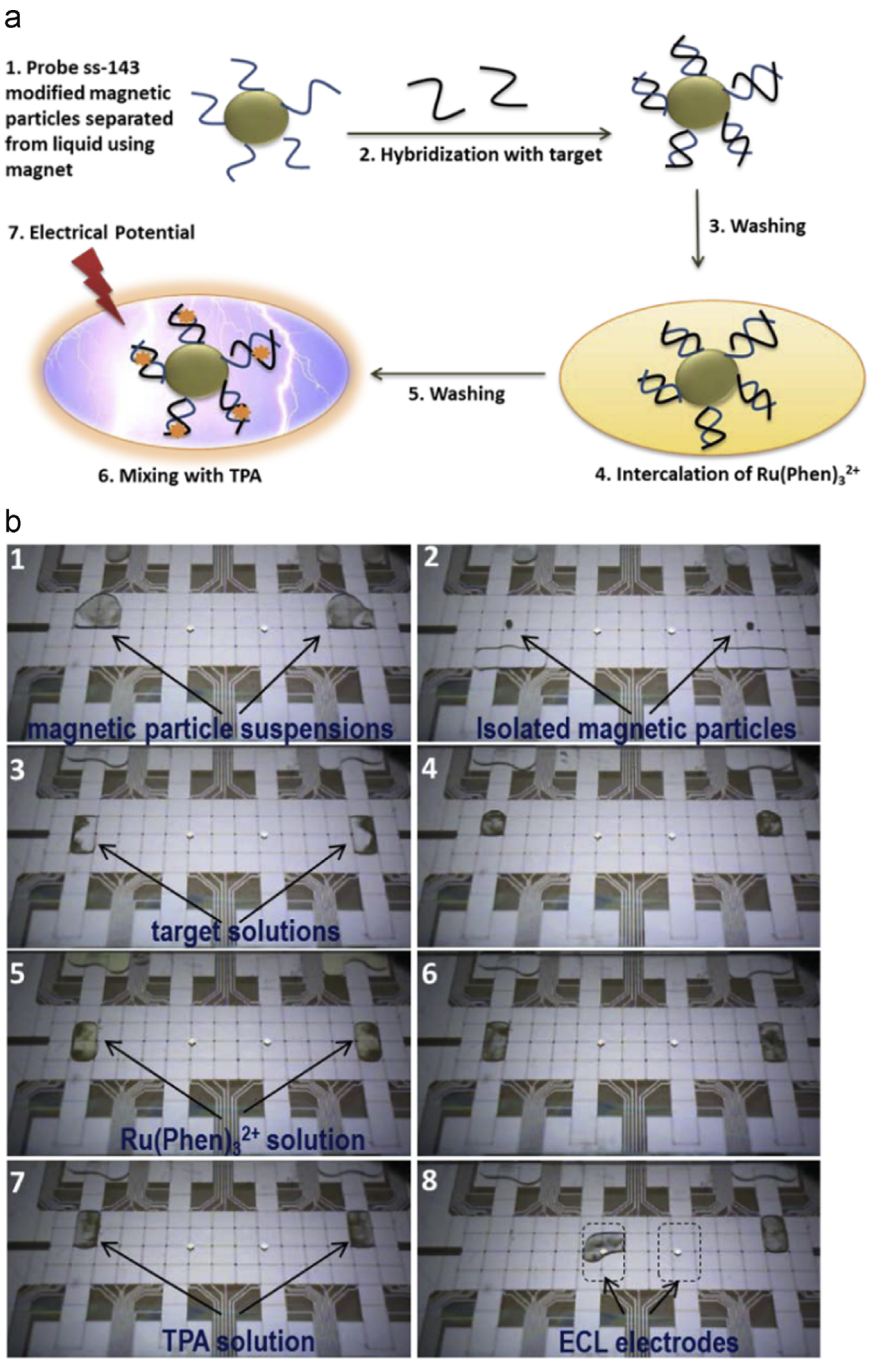

Fig. 3. DMF-ECL oligonucleotide hybridization assay. (a) Schematic depicting the seven-step DMF protocol developed to detect miRNA-143 by electrochemiluminescence (ECL). (b) Frames from a movie depicting the running of two protocols in parallel: (1&2) droplets of ss-143-modified beads are dispensed onto the main platform from reservoir electrodes, followed by magnetic separation of the particles from solution, (3&4) particles are incubated with target sequence droplet followed by wash steps, (5&6) particles are incubated with $Ru(Phen)_3^{2+}$ solution followed by wash steps, (7) particles are mixed with TPA solution, and (8) finally, one of the two droplets (on the left) is actuated to the ITO WE and Ag/Au/ITO-CE/RE (area inside the dotted rectangle) to measure the ECL. The droplet on the right is queued for a subsequent measurement.

Fig. 4b shows the relative ECL responses of the various sequences. It is evident that single and double nucleotide mismatched sequences can be distinguished from fully complementary sequence ($p=0.002$, $p=0.001$ respectively), an effect of (1) the decrease in hybridization efficiency and (2) structural distortion(s) in the double helix. For the former (1), reduction in hybridization efficiency is enhanced (increasing selectivity) for surface-bound probes relative to free probes in solution because of steric limitations (Shamsi and Kraatz, 2013). For the latter (2), structural distortions decrease the level of intercalation of $Ru(phen)_3^{2+}$. Combined, these two effects increase with multiple nucleotide mismatches (Shamsi and Kraatz, 2011), which is evident in the significant differences between the signals observed for 143-m1 and 143-m2 ($p=0.005$). Finally, the signal from the fully non-complementary sequence cannot be distinguished from that of the blank ($p=0.2$). Taken together, these data suggest that the new technique is quite selective.

The quantitative performance of the new system was assessed by evaluating a dilution series of the complementary target, ds-143. Fig. 5a is a calibration curve for these experiments comprising 0, 10, 100, and 1000 nM target concentrations (with CVs of 82%, 16%, 26%, and 16% respectively) with concentration limit of

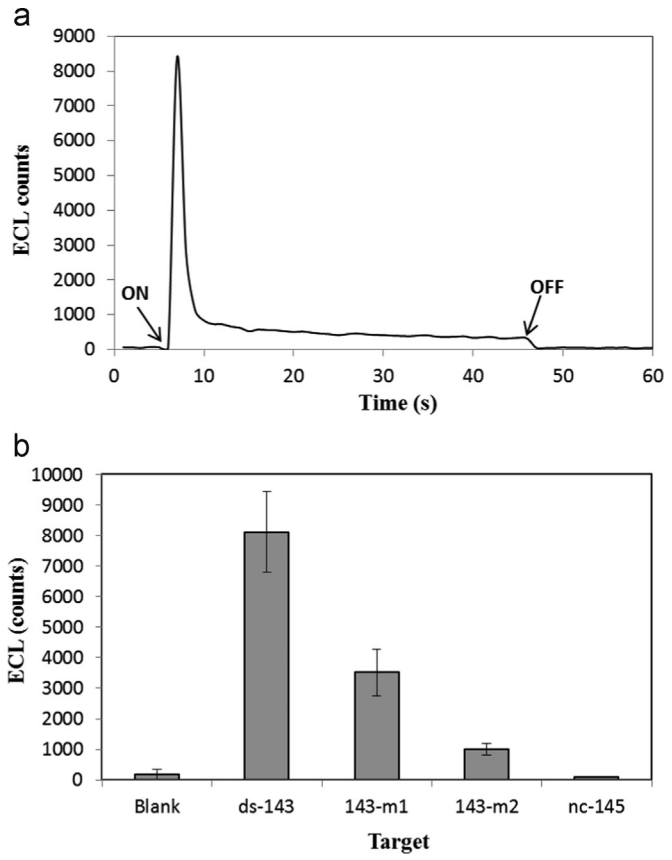

Fig. 4. DMF-ECL DNA hybridization efficiency. (a) Representative ECL response of ds-143-bound $[Ru(Phen)_3]^{2+}$ on magnetic beads in TPA. ITO (WE) and Ag/Au/ITO (CE/RE).The "ON" and "OFF" labels indicate when 1.5 V DC was applied and removed between the ITO WE and the Ag/Au/ITO CE/RE. (b) Average response of blank (no target), fully complementary ds-143, single nucleotide mismatched 143-m1, double nucleotide mismatch 143-m2, and fully non-complementary nc-145. In each case, the target concentration was 1 μM, the data represent the average of 4 replicates, and the error bars represent +/− one standard deviation.

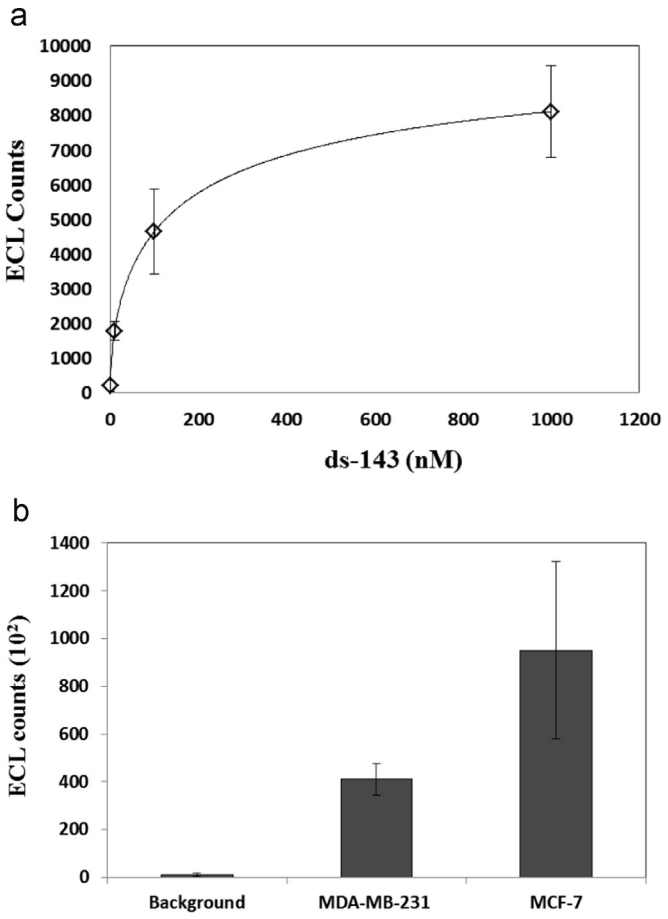

Fig. 5. DMF-ECL for quantitation and evaluation of cell lysate. (a) ECL signal as a function of ds-143 concentration. (b) ECL signal background (generated from cell media), and in MDA-MB-231 and MCF-7 cell lysates generated from 10^6 cell/mL suspensions. All data represent the average of 4 replicates, and the error bars represent +/− one standard deviation.

detection of C_{LOD} = 1.1 nM and absolute LOD = 1.5 femtomoles. This performance is suitable for the application of interest here (analysis of cell lysate, described below), but may not be sufficient to quantify miRNA-143 in human blood or serum. If greater sensitivity is needed in future applications, the limit of detection might be improved by optimizing WE area, optical filters, and other parameters (as described above), or ECL-DMF might be integrated with digital microfluidic methods designed to pre-concentrate RNA from large volumes of blood (Jebrail et al., 2014) prior to analysis.

3.3. Detection of miRNA in tumor cells using DMF-ECL

Finally, motivated by the intense interest in microRNA expression profiles in cancer cells (Turchinovich et al., 2011), we applied the new DMF-ECL method to evaluating miRNA-143 expression in two cancer cell lines. Fig. 5b shows the signals observed for cell-density-matched samples of lysate collected from MDA-MB-231 and MCF-7 cell lines. As shown, the signals observed for both MDA-MB-231 (41,000 +/−6,500) and MCF-7 (95,000 +/− 37,100) are greater than that of the background (17,000 +/−8,000). Note that the variances on these measurements are relatively high (i.e., CVs of 16% and 39% for MD-MB-231 and MCF-7, respectively), likely caused by the inherent variabilities that are often observed in proliferating cancer cells. But even with this level of error, the ECL signal observed for MDA-MB-231 is significantly lower than that observed for MCF-7 (p = 0.03). This observation is consistent with the understanding that miRNA-143 expression is down-regulated in some aggressive forms of cancer (Ng et al., 2009), and that MDA-MB-231 cells are the more aggressive (in terms of propensity to metastasize) of the two lines evaluated here (Weigel et al., 2010).

4. Conclusion

We report the first integration of electroluminescence detection with digital microfluidics. The method was validated by application to magnetic particle-based nucleic acid hybridization assays using sample volumes of 1.8 μL. The system can specifically detect single nucleotide differences in 21-mer deoxyribose analogues of miRNA-143, with a limit of detection of 1.5 femtomoles. Moreover, the system is capable of detecting microRNA in breast cancer cell lysates, allowing for the discrimination between cell type.

Acknowledgment

We thank the Canadian Institutes for Health Research (CIHR) (Grant no. 111625), the National Science and Engineering Research Council (NSERC) (Grant no. RGPIN 2014-06042), and Abbott Diagnostics for support. A.R.W. thanks the Canada Research Chair

(CRC) Program for a CRC.

Appendix A. Supplementary material

Supplementary material associated with this article can be found in the online version at doi:10.1016/j.bios.2015.10.036.

References

Arora, A., Eijkel, J.C.T., Morf, W.E., Manz, A., 2001. A Wireless electrochemiluminescence detector applied to direct and indirect detection for electrophoresis on a microfabricated glass device. Anal. Chem. 73 (14), 3282–3288.

Au, S.H., Kumar, P., Wheeler, A.R., 2011. A New angle on pluronic additives: advancing droplets and understanding in digital microfluidics. Langmuir 27 (13), 8586–8594.

Azimi, M., Silverbrook, K., Moini, A., 2011. Microfluidic device for detection of nucleic acid targets with electrochemiluminescent probes. US 20110312642.

Calin, G.A., Croce, C.M., 2006. MicroRNA signatures in human cancers. Nat. Rev. Cancer 6 (11), 857–866.

Cao, W., Liu, J., Yang, X., Wang, E., 2002. New technique for capillary electrophoresis directly coupled with end-column electrochemiluminescence detection. Electrophoresis 23, 3683–3691.

Chen, Y., Xu, J., Su, J., Xiang, Y., Yuan, R., Chai, Y., 2012. In situ hybridization chain reaction amplification for universal and highly sensitive electrochemiluminescent detection of DNA. Anal. Chem. 84 (18), 7750–7755.

Chiang, M.T., Whang, C.W., 2001. Tris(2,2'-bipyridyl)ruthenium(III)-based electrochemiluminescence detector with indium/tin oxide working electrode for capillary electrophoresis. J. Chromatogr. A 934 (1–2), 59–66.

Choi, K., Ng, A.H.C., Fobel, R., Chang-Yen, D.A., Yarnell, L.E., Pearson, E.L., Oleksak, C. M., Fischer, A.T., Luoma, R.P., Robinson, J.M., Audet, J., Wheeler, A.R., 2013. Automated digital microfluidic platform for magnetic-particle-based immunoassays with optimization by design of experiments. Anal. Chem. 85 (20), 9638–9646.

Choi, K., Mudrik, J.M., Wheeler, A.R., 2015. A Guiding Light: Spectroscopy on Digital Microfluidic Devices Using in-Plane Optical Fibre Waveguides. Anal. Bioanal. Chem. 407 (24), 7467–7475.

Choi, K., Ng, A.H.C., Fobel, R., Wheeler, A.R., 2012. Digital microfluidics. Annu. Rev. Anal. Chem. 5 (1), 413–440.

Delaney, J.L., Hogan, C.F., Tian, J., Shen, W., 2011. Electrogenerated chemiluminescence detection in paper-based microfluidic sensors. Anal. Chem. 83 (4), 1300–1306.

Dryden, M.D.M., Rackus, D.D.G., Shamsi, M.H., Wheeler, A.R., 2013. Integrated digital microfluidic platform for voltammetric analysis. Anal. Chem. 85 (18), 8809–8816.

Dryden, M.D.M., Wheeler, A.R., 2015. DStat: a versatile, open-source potentiostat for electroanalysis and integration. PLoS One . http://dx.doi.org/10.1371/journal.pone.0140349.

Fobel, R., Fobel, C., Wheeler, A.R., 2013. DropBot: an open-source digital microfluidic control system with precise control of electrostatic driving force and instantaneous drop velocity measurement. Appl. Phys. Lett. 102 (19), 1–5.

Foudeh, A.M., Brassard, D., Tabrizian, M., Veres, T., 2015. Rapid and multiplex detection of Legionella's RNA using digital microfluidics. Lab Chip 15 (6), 1609–1618.

Ge, L., Yan, J., Song, X., Yan, M., Ge, S., Yu, J., 2012. Three-dimensional paper-based electrochemiluminescence immunodevice for multiplexed measurement of biomarkers and point-of-care testing. Biomaterials 33 (4), 1024–1031.

Guan, W., Liu, M., Zhang, C., 2016. Electrochemiluminescence detection in microfluidic cloth-based analytical devices. Biosens. Bioelectron. 75, 247–253.

Hsueh, Y.T., Collins, S.D., Smith, R.L., 1998. DNA quantification with an electrochemiluminescence microcell. Sens. Actuators B: Chem. 49, 1–4.

Hsueh, Y.T., Smith, R.L., Northrup, M.A., 1996. A microfabricated, electrochemiluminescence cell for the detection of amplified DNA. Sens. Actuators B: Chem. 33 (1–3), 110–114.

Hu, L., Xu, G., 2010. Applications and trends in electrochemiluminescence. Chem. Soc. Rev. 39 (8), 3275–3304.

Jebrail, M.J., Sinha, A., Vellucci, S., Renzi, R.F., Ambriz, C., Gondhalekar, C., Schoeniger, J.S., Patel, K.D., Branda, S.S., 2014. World-to-digital-microfluidic interface enabling extraction and purification of RNA from human whole blood. Anal. Chem. 86 (8), 3856–3862.

Kasahara, T., Matsunami, S., Edura, T., Ishimatsu, R., Oshima, J., Tsuwaki, M., Imato, T., Shoji, S., Adachi, C., Mizuno, J., 2014. Multi-color microfluidic electrochemiluminescence cells. Sens. Actuators A: Physical 214, 225–229.

Kokalj, T., Pérez-Ruiz, E., Lammertyn, J., 2015. Building bio-assays with magnetic particles on a digital microfluidic platform. New Biotechnol. 32 (5), 485–503.

Labib, M., Berezovski, M.V., 2015. Electrochemical sensing of microRNAs: Avenues and paradigms. Biosens. Bioelectron. 68, 83–94.

Lafrenière, N.M., Shih, S.C.C., Abu-Rabie, P., Jebrail, M.J., Spooner, N., Wheeler, A.R., 2014. Multiplexed extraction and quantitative analysis of pharmaceuticals from DBS samples using digital microfluidics. Bioanalysis 6 (3), 307–318.

Li, Y., Huang, C., Zheng, J., Qi, H., Cao, W., Wei, Y., 2013. Label-free electrogenerated chemiluminescence biosensing method for trace bleomycin detection based on a Ru $(phen)_3^{2+}$ hairpin DNA composite film electrode. Biosens. Bioelectron. 44, 177–182.

Liu, D.-Y.Y., Xin, Y.-Y.Y., He, X.-W.W., Yin, X.-B.B., 2011. A sensitive, non-damaging electrochemiluminescent aptasensor via a low potential approach at DNA-modified gold electrodes. Analyst 136 (3), 479–485.

Liu, R., Zhang, C., Liu, M., 2015. Open bipolar electrode-electrochemiluminescence imaging sensing using paper-based microfluidics. Sens. Actuators B: Chem. 216, 255–262.

Mani, V., Kadimisetty, K., Malla, S., Joshi, A.A., Rusling, J.F., 2013. Paper-based electrochemiluminescent screening for genotoxic activity in the environment. Environ. Sci. Technol. 47 (4), 1937–1944.

Miao, W., 2008. Electrogenerated chemiluminescence and its biorelated applications. Chem. Rev. 108 (7), 2506–2553.

Miao, W., Choi, J.-P., Bard, A.J., 2002. Electrogenerated Chemiluminescence 69: The Tris(2,2'-bipyridine)ruthenium(II), $(Ru(bpy)_3^{2+})$/Tri-n-propylamine (TPrA) System RevisitedA New Route Involving $TPrA^{\bullet+}$ Cation Radicals. J. Am. Chem. Soc. 124, 14478–14485.

Mirasoli, M., Guardigli, M., Michelini, E., Roda, A., 2014. Recent advancements in chemical luminescence-based lab-on-chip and microfluidic platforms for bioanalysis. J. Pharm. Biomed. Anal. 87, 36–52.

Muzyka, K., 2014. Current trends in the development of the electrochemiluminescent immunosensors. Biosens. Bioelectron. 54, 393–407.

Nepomnyashchii, A.B., Bard, A.J., Leland, J.K., Debad, J.D., Sigal, G.B., Wilbur, J.L., Wohlstadter, J.N., 2006. Chemiluminescence, Electrogenerated. Encyclopedia of Analytical Chemistry. John Wiley & Sons, Ltd..

Ng, A.H.C., Choi, K., Luoma, R.P., Robinson, J.M., Wheeler, A.R., 2012. Digital microfluidic magnetic separation for particle-based immunoassays. Anal. Chem. 84 (20), 8805–8812.

Ng, A.H.C., Lee, M., Choi, K., Fischer, A.T., Robinson, J.M., Wheeler, A.R., 2015. Digital microfluidic platform for the detection of rubella infection and immunity: a proof of concept. Clin. Chem. 61, 420–429.

Ng, E.K.O., Tsang, W.P., Ng, S.S.M., Jin, H.C., Yu, J., Li, J.J., Rocken, C., Ebert, M.P.A., Kwok, T.T., Sung, J.J.Y., 2009. MicroRNA-143 targets DNA methyltransferases 3A in colorectal cancer. Br. J. Cancer 101 (4), 699–706.

Parveen, S., Aslam, M., Hu, L., Xu, G., 2013. Electrogenerated Chemiluminescence: Protocols and Applications. Springer, Berlin, Heidelberg.

Rackus, D.G., Shamsi, M.H., Wheeler, A.R., 2015. Electrochemistry, biosensors and microfluidics: a convergence of fields. Chem. Soc. Rev. 44, 5320–5340.

Radha, P., Mark, M.R., 2007. ECL—Electrochemical luminescence. Annu. Rep. Section "C" (Physical Chemistry) 103, 12–78.

Redha, Z.M., Baldock, S.J., Fielden, P.R., Goddard, N.J., Brown, B.J.T., Haggett Barry, G. D., Andres, R., Birch, B., J., 2009. Hybrid microfluidic sensors fabricated by screen printing and injection molding for electrochemical and electrochemiluminescence detection. Electroanalysis 21, 422–430.

Richter, M.M., 2004. Electrochemiluminescence (ECL). Chem. Rev. 104 (6), 3003–3036.

Robert, J.F., Paolo, B., Tia, E.K., 2009. Electrogenerated Chemiluminescence. Annu. Rev. Anal. Chem. 2, 359–385.

Sardesai, N.P., Barron, J.C., Rusling, J.F., 2011. Carbon nanotube microwell array for sensitive electrochemiluminescent detection of cancer biomarker proteins. Anal. Chem. 83 (17), 6698–6703.

Sardesai, N.P., Kadimisetty, K., Faria, R., Rusling, J.F., 2013. A microfluidic electrochemiluminescent device for detecting cancer biomarker proteins. Anal. Bioanal. Chem. 405 (11), 3831–3838.

Shamsi, M., Kraatz, H.-B., 2013. Interactions of metal ions with DNA and some applications. J. Inorg. Organomet. Polym. 23 (1), 4–23.

Shamsi, M.H., Choi, K., Ng, A.H.C., Wheeler, A.R., 2014. A digital microfluidic electrochemical immunoassay. Lab on a chip 14, 547–554.

Shamsi, M.H., Kraatz, H.-B., 2011. Electrochemical identification of artificial oligonucleotides related to bovine species. Potential for identification of species based on mismatches in the mitochondrial cytochrome C1 oxidase gene. Analyst 136 (22), 4724–4731.

Silverbrook, K., Azimi, M., Facer, G.R., 2011. Microfluidic device for PCR, probe hybridization and electrochemiluminescent detection of probe-target hybrids. US 20110312655.

Skotty, D.R., Lee, W.Y., Nieman, T.A., 1996. Determination of dansyl amino acids and oxalate by HPLC with electrogenerated chemiluminescence detection using tris (2, 2′-bipyridyl) ruthenium (II) in the mobile Phase. Anal. Chem. 68, 1530–1535.

Tokel-Takvoryan, N.E., Hemingway, R.E., Bard, A.J., 1973. Electrogenerated chemiluminescence. XIII. Electrochemical and electrogenerated chemiluminescence studies of ruthenium chelates. J. Am. Chem. Soc. 95 (20), 6582–6589.

Tsaloglou, M.-N., Jacobs, A., Morgan, H., 2014. A fluorogenic heterogeneous immunoassay for cardiac muscle troponin cTnI on a digital microfluidic device. Anal. Bioanal. Chem. 406 (24), 5967–5976.

Turchinovich, A., Weiz, L., Langheinz, A., Burwinkel, B., 2011. Characterization of extracellular circulating microRNA. Nucleic Acids Res. 39 (16), 7223–7233.

Wang, S., Ge, L., Zhang, Y., Song, X., Li, N., Ge, S., Yu, J., 2012. Battery-triggered microfluidic paper-based multiplex electrochemiluminescence immunodevice based on potential-resolution strategy. Lab on a chip 12 (21), 4489–4498.

Weigel, M., Dahmke, L., Schem, C., Bauerschlag, D., Weber, K., Niehoff, P., Bauer, M., Strauss, A., Jonat, W., Maass, N., Mundhenke, C., 2010. In vitro effects of imatinib mesylate on radiosensitivity and chemosensitivity of breast cancer cells. BMC Cancer 10 (1), 412.

Welch, E.R.F., Lin, Y.Y., Madison, A., Fair, R.B., 2011. Picoliter DNA sequencing chemistry on an electrowetting-based digital microfluidic platform. Biotechnol.

J. 6, 165–167.
Woolley, A.T., 2015. ABC Spotlight on emerging microRNA analysis methods. Anal. Bioanal. Chem. 407 (22), 6579–6581.
Wu, M.-S., Liu, Z., Shi, H.-W., Chen, H.-Y., Xu, J.-J., 2015. Visual Electrochemiluminescence detection of cancer biomarkers on a closed bipolar electrode array chip. Anal. Chem. 87, 530–537.
Xu, X.H., Bard, A.J., 1995. Immobilization and hybridization of DNA on an aluminum (III) alkanebisphosphonate thin film with electrogenerated chemiluminescent detection. J. Am. Chem. Soc. 117, 2627–2631.
Yan, J., Yan, M., Ge, L., Yu, J., Ge, S., Huang, J., 2013. A microfluidic origami electrochemiluminescence aptamer-device based on a porous Au-paper electrode and a phenyleneethynylene derivative. Chem. Commun. 49 (14), 1383–1385.
Yin, X.-B., Dong, S., Wang, E., 2004. Analytical applications of the electrochemiluminescence of tris (2,2′-bipyridyl) ruthenium and its derivatives. TrAC Trends Anal. Chem. 23 (6), 432–441.
Yin, X.-B., Xin, Y.-Y., Zhao, Y., 2009. Label-Free electrochemiluminescent aptasensor with attomolar mass detection limits based on a $Ru(phen)_3^{2+}$-double-strand DNA composite film electrode. Anal. Chem. 81 (22), 9299–9305.
Zhang, Y., Liu, W., Ge, S., Yan, M., Wang, S., Yu, J., Li, N., Song, X., 2013. Multiplexed sandwich immunoassays using flow-injection electrochemiluminescence with designed substrate spatial-resolved technique for detection of tumor markers. Biosens. Bioelectron. 41, 684–690.